https://doi.org/10.5194/egusphere-2025-6368
Preprint. Discussion started: 18 February 2026

Revisiting the Parameterization of Ice Nucleation of Dust Particles under Mixed-Phase Cloud Conditions from Laboratory Measurements

Jie Chen[1,*] and Zamin A. Kanji[1,*]

[1]Institute for Atmospheric and Climate Science, ETH Zürich, Zurich, 8092, Switzerland

Correspondence to: jie.chen@env.ethz.ch and zamin.kanji@env.ethz.ch

Abstract. Dust aerosol plays a key role in cloud formation and evolution due to its high atmospheric abundance and efficient ice nucleation abilities (INA). However, a generalized parameterization of dust-induced ice formation in climate models remains challenging, because dust INA varies substantially with mineral composition, measurement methods, and atmospheric aging processes. In this study, we revisited the INA of dust particles under mixed-phase cloud conditions (MPC, -38 < T < 0 °C) compiled from previous laboratory studies. Our results indicate that measurement methods, whether particles are dry-dispersed or wet-suspended introduce the largest variability in reported dust INA, represented by n_s (ice active site surface density), showing a difference of 1−6 orders of magnitude at -38 < T < -18 °C. This discrepancy likely arises from different water-particle interactions between the two methods, including particle coagulation at artificially high particle concentration and surface modification by water. Aging generally reduces dust INA, with chemical reactions inducing the strongest reduction, followed by thermal treatments and water/aqueous aging. Based on these findings, we developed a suite of n_s −based parameterizations to represent INA of dust particles with mixed and specific mineral composition. To overcome the variability introduced by measurement methods, we also developed parameterizations based on D_e (spherical equivalent particle diameter within a droplet), which predict droplet freezing across the full MPC temperature range using a single expression. The developed parameterizations provide a physically grounded approach for representing dust INA and are expected to improve the accuracy of predictions of dust-induced cloud formation in climate models.

Keywords

Ice nucleation, dust particles, ice nucleation parameterizations

1. Introduction

Aerosol particles can trigger ice formation from liquid water or water vapor in the atmosphere by serving as ice nucleating particles (INPs), a process known as heterogeneous ice

https://doi.org/10.5194/egusphere-2025-6368
Preprint. Discussion started: 18 February 2026

nucleation. Unlike homogeneous freezing of cloud droplets in the absence of an INP (T < -38 °C), heterogeneous ice nucleation occurs at less extreme temperatures (T > -38 °C) and lower ice supersaturation conditions. This difference arises because INPs provide a surface that lowers the energy barrier required for forming critical ice embryos. Heterogeneous ice nucleation is particularly important for mixed-phase clouds (MPCs), where homogeneous freezing rates are too low at $T \gtrsim$ -38 °C. Quantifying aerosol ice nucleation is therefore fundamental for predicting cloud phase, precipitation and radiative properties (Burrows et al., 2022; Murray et al., 2021). The physicochemical properties and ice nucleation ability (INA) of INPs vary with their emission sources and can be modified by complex atmospheric aging processes (Kanji et al., 2017). This variability complicates the identification of ice nucleation mechanisms of INPs and the parameterization of their ice formation in climate models, limiting our ability to simulate aerosol–cloud interactions and their climate impacts (Burrows et al., 2022; Murray et al., 2021; Mcgraw et al., 2023).

Over the past three decades, significant progress has been made in characterizing the INA of atmospherically relevant INP species, as reviewed by many studies (Hoose and Möhler, 2012; Kanji et al., 2017; Murray et al., 2012; Huang et al., 2021). Among these species, mineral dust originating from desert, arid soil and volcanic sources are considered the most important INPs, due to the high atmospheric abundance and generally strong INA under MPC relevant conditions (T < -8 °C), as reported by numerous field and laboratory studies (Hoose and Möhler, 2012; Kanji et al., 2017; Murray et al., 2012). Based on these experimental findings, ice formation parameterizations have been developed to represent the INA of dust particles. Table S1 summarizes existing parameterizations derived from immersion freezing measurements of dust particles. Immersion freezing is considered the dominant ice nucleation pathway in MPCs (Ansmann et al., 2008; De Boer et al., 2011), in which an INP is immersed within a supercooled droplet and triggers droplet freezing. In general, two major types of parameterization approach have been developed: (i) classical nucleation theory (CNT)-based parameterizations (Marcolli et al., 2007; Chen et al., 2008; Murray et al., 2011; Niedermeier et al., 2011a; Savre and Ekman, 2015), which estimate heterogeneous ice nucleation rates (J_{het}, Table S1) of INPs based on environmental variables (e.g., temperature and ice saturation) and the contact angle (θ) between the ice embryo and INP surface (Chen et al., 2008; Savre and Ekman, 2015; Niedermeier et al., 2011a; Marcolli et al., 2007; Murray et al., 2011). The contact angle was determined based on surface properties of aerosol particles, and different assumptions were therefore made across

https://doi.org/10.5194/egusphere-2025-6368
Preprint. Discussion started: 18 February 2026

studies. More details can be found in Table S1. (ii) empirical parameterizations (Demott et al., 2010; Demott et al., 2015; Chen et al., 2024), which relate INP concentrations to physicochemical properties of aerosol particles, such as size distribution and surface area. For example, previous studies developed parameterizations to predict INP concentrations based on the number of dust aerosol particles larger than 500 nm (Demott et al., 2010; Demott et al., 2015) or 1 μm (Mignani et al., 2021; Chen et al., 2024), by observing a strong correlation between these two variables. Another widely used parameter is the active site density of dust particles, which assumes that ice nucleation is triggered by active sites located on the particle surface. A greater number of active sites corresponds to a higher probability of particles forming ice. To enable comparison across different particle types and experimental conditions, the number of active sites is typically normalized by particle surface area or mass, resulting in the active site surface density (n_s) and mass density (n_m), respectively. Parameterizations are developed accordingly by fitting the temperature dependency of n_s or n_m (listed in Table S1). INP concentration in the atmosphere can then be estimated from n_s or n_m if particle size distribution or mass is known. As summarized in Table S1, most existing dust INP parameterizations are derived either from a single study or from measurements on individual mineral species. Although some studies measured natural dust with complex composition, they are often restricted to samples collected from certain locations (Kanji et al., 2019; Boose et al., 2016). In addition, most parameterizations are constrained to narrow temperature ranges (Table S1), largely due to the detection limits of utilized ice nucleation techniques. As a result, current parameterizations may not adequately capture the variability of dust INA under atmospherically relevant conditions, where particles exhibit diverse mineral compositions and nucleate ice across a wide range of MPC temperatures. Parameterizations capable of representing dust INA from multiple sources and across the full MPC temperature range are required.

Experimental methods also contribute to discrepancies in reported INA of dust particles (Hiranuma et al., 2015; Emersic et al., 2015; Demott et al., 2018). Two common aerosol generation techniques used in the laboratory for immersion freezing studies (Hiranuma et al., 2015; Emersic et al., 2015; Demott et al., 2018) are: dry dispersion of aerosol particles, typically measured using ice nucleation chambers, and wet suspension of particles using droplet freezing techniques (DFTs). Hiranuma et al. (2015) compared INA of illite particles measured by 17 different instruments and found that n_s values measured by dry and wet generation techniques differed by up to 3 orders of magnitude. They attributed this discrepancy to surface changes in

https://doi.org/10.5194/egusphere-2025-6368
Preprint. Discussion started: 18 February 2026

particles induced by water interactions, such as ion dissolution, which are likely more pronounced in wet suspensions (DFTs). Similarly, Emersic et al. (2015) observed higher n_s values for illite and kaolinite particles when measured using a cloud chamber compared to DFTs. They proposed an alternative explanation that dust particles may coagulate in suspension, thereby reducing the effective particle surface area available for ice nucleation. These studies point to the importance of particle–water interactions in determining the INA of dust particles. In dry dispersion and wet suspension measurements, the methodological differences in concentration and water contact time of particles may influence such interactions and contribute to variations in dust INA, an aspect that remains poorly quantified and constrained.

Atmospheric aging of dust particles, including chemical reactions with trace gases and aqueous interactions with water or salt solutions, further modifies the INA of dust particles (Huang et al., 2025; Kanji et al., 2017). The aging effects can vary with both mineral composition and aging pathways. For example, montmorillonite (Salam et al., 2007; Salam et al., 2008) and K-feldspar (Kumar et al., 2018; Chen et al., 2023a; Kumar et al., 2019a) exhibit enhanced INA after exposure to ammonia (NH_3) gas or NH_3/NH_4^+ solutions. In contrast, Kumar et al. (2019a) indicated that the INA of quartz is decreased in alkaline solutions, which may be caused by the increased dissolution of quartz under alkaline conditions. Chemical aging or coating of dust particles (e.g., natural desert dust (Kanji et al., 2019), Arizona Test Dust (Knopf and Koop, 2006; Sullivan et al., 2010; Niedermeier et al., 2011b), illite (Kulkarni et al., 2014; Augustin-Bauditz et al., 2014), kaolinite (Tobo et al., 2012; Wex et al., 2014; Augustin-Bauditz et al., 2014) and feldspar (Augustin-Bauditz et al., 2014; Kulkarni et al., 2014)) with acids and organic aerosol, leads to a reduction in their INA. Harrison et al. (2019) indicate that the INA of certain quartz species remains unchanged even after months of immersion in water or salt solutions. These results highlight the complexity and composition-specific nature of dust aging, suggesting that both dust type and aging pathway need to be considered when developing parameterizations for representing INA of aged dust particles.

In general, previous studies suggest that accounting for dust composition, atmospheric aging effects, and uncertainties related to measurement methods is important for interpreting the INA of dust particles and accurately representing their ice nucleation by parameterizations. In this work, we revisit the INA of dust particles reported for -38< T < 0 °C, above water saturation (i.e., MPC conditions) using data compiled from previous laboratory studies. Specifically, we assessed the influence of mineral aerosol composition, generation methods and

https://doi.org/10.5194/egusphere-2025-6368
Preprint. Discussion started: 18 February 2026

simulated aging pathways on INA of dust particles. Based on our findings, we propose revised empirical mineral dust INP parameterizations valid for immersion freezing throughout the MPC temperature range, accounting for measurement methods and aging pathways.

2. Methodology

2.1 Data collection

The ice nucleation data for mineral dust particles were compiled from 25 published laboratory studies conducted between 2007 and 2023, as summarized in Table S2. These studies were identified through keyword-based searches in *Web of Science* and *Google Scholar*. The datasets combined digitized data from figures in literature, open-access repositories, and directly from corresponding authors (see Acknowledgments for details). All data included in our work were published, no unpublished data were considered.

The collected studies focused on the INA of dust particles in the immersion mode with diverse mineral compositions, subjected to varied aging treatments, and generated and measured using both dry-dispersion and wet-suspension methods. Specifically, the dust particles investigated include natural dust from desert and volcanic sources, as well as particles composed mainly of nominally single mineral species, such as illite, quartz, kaolinite, feldspar, and montmorillonite. Ice formation data for Arizona Test Dust (ATD, Powder Technology Inc.) are also included, a formerly widely used surrogate of atmospheric dust in ice nucleation research. Soil dust particles from agricultural sources were excluded, due to their substantially different INA compared to desert and volcanic dust, resulting from their higher organic content and will be addressed in a separate study. In laboratory measurements, dust particles were subjected to various chemical and physical treatments to mimic their atmospheric aging and to evaluate the associated impacts on their INA. These treatments included immersion in water or salt and acid solutions (hereafter referred to as water aging and aqueous aging), thermal treatment, and chemical aging either through exposure to reactive gases or through coating with inorganic and organic acids or secondary organic aerosol (hereafter referred to as gas chemical aging and coating). More details about the aging treatments can be found in Table S1.

2.2 Metrics to quantify INA of immersion mode dust particles

Different ice nucleation metrics have been established to quantify and compare INA of dust particles, as summarized by Kanji et al. (2017). In this work, we use n_s to compare the INA of different dust types and to develop primary ice nucleation parameterizations. This

https://doi.org/10.5194/egusphere-2025-6368
Preprint. Discussion started: 18 February 2026

choice is motivated by several advantages. n_s is an aerosol-aware metric that accounts for particle size and surface characteristics, which aids the mechanistic interpretation of dust INA based on aerosol physicochemical properties. Compared to other available metrics (e.g., n_m), n_s has the most extensive data coverage among the collected studies, enabling broader and more consistent cross-comparisons. In addition, n_s can be readily incorporated into climate models to predict the number of ice crystals induced by dust INPs, if particle size (i.e., surface area) is known. The following equations illustrate how n_s can be derived based on ice nucleation measurements using different methods, i.e., chamber experiments with dry-dispersed aerosol and DFTs with wet-suspended particles. n_s assumes a strong temperature dependence and time is neglected because of the secondary importance of time compared to temperature for dust particles (Welti et al., 2012; Kanji et al., 2013; Budke and Koop, 2015; Wright and Petters, 2013; Vali and Snider, 2015).

Dry-dispersed aerosol (chamber experiments):

$$n_s(T) = \frac{-\ln(1 - AF)}{S_p} \quad (1)$$

$$AF = \frac{N_{\text{ice crystals}}(T)}{N_{\text{total particles}}} \quad (2)$$

Here, AF (Eq. (2)) is the ice activated fraction of aerosol particles, which is calculated based on the number of formed ice crystals ($N_{\text{ice crystals}}$) and total number of aerosol particles ($N_{\text{total particles}}$) measured in the chamber experiments. S_p (Eq. (1)) represents the surface area of a single aerosol particle.

Wet-suspended particles (DFT experiments):

$$n_s(T) = \frac{-\ln(1 - FF)}{S_d} \quad (3)$$

$$FF = \frac{N_{\text{frozen droplets}}(T)}{N_{\text{total droplets}}} \quad (4)$$

Here, FF (Eq. (4)) is the frozen fraction of droplets determined from the number of frozen droplets ($N_{f\text{rozen droplets}}$) and total number of detected droplets ($N_{\text{total droplets}}$) in the droplet freezing measurements. S_d (Eq. (3)) represents the surface area of particles immersed within a droplet.

https://doi.org/10.5194/egusphere-2025-6368
Preprint. Discussion started: 18 February 2026

To account for the stochastic nature (time dependence) of ice nucleation, the **time dependent metrics**—heterogeneous ice nucleation rate (J_{het}, m^{-2} s^{-1}), can be calculated based on following equations for dry-dispersed aerosol (Eq. (5)) and wet-suspended particles (Eq. (6)), respectively.

$$J_{het,\ dry} = \frac{n_s(T)}{t} \quad (5)$$

$$J_{het,\ wet} = \frac{-\ln\left(1 - \frac{\Delta N_{frozen}}{N_{unfrozen}}\right)}{s_d \Delta t} \quad (6)$$

Here, J_{het} describes the number of nucleation events per unit particle surface and unit time. In chamber experiments, $J_{het,dry}$ is derived based on the residence time (t) of aerosol particles exposed to ice formation conditions (Eq. (5)). In DFT measurements ($J_{het,wet}$, Eq. (6)), ΔN_{frozen} denotes the number of droplets that freeze within the time interval Δt from t_1 to t_2. $N_{unfrozen}$ is the number of droplets that remain unfrozen at time t_1. Δt can be calculated based on the reported cooling rate in each freezing experiment. The residence time of aerosol particles in chamber measurements or the cooling rates in DFTs used in each study are provided in Table S2. We note that the practice of using chamber residence times slightly underestimates $J_{het,dry}$ because the residence time is larger than the nucleation time.

3 Results and discussions

3.1 The INA of dust particles with different compositions

A compilation of n_s values of dust particles with different mineral compositions is shown in Figure 1. n_s values exhibit substantial variability across the studied temperature range (-42 < T < -2 °C), for example, at T = -20 °C, n_s spans 7 orders of magnitude ranging from 5.0×10^3 to 1.7×10^{11} m^{-2}. This variability likely arises from multiple factors, including dust composition, measurement methods and aging processes, we therefore conduct a more detailed investigation into these aspects below.

https://doi.org/10.5194/egusphere-2025-6368
Preprint. Discussion started: 18 February 2026

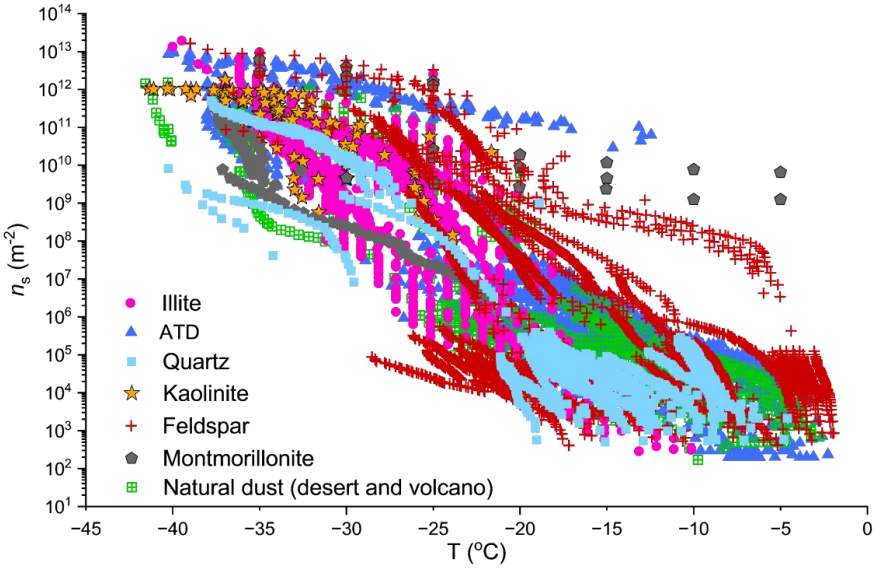

Figure 1. The INA of dust particles with different mineral compositions, represented by the ice active site surface density (n_s). The dust species included in our analysis are illite (pink, circle), Arizona Test Dust (ATD, dark blue, triangle), quartz (light blue, square), kaolinite (orange, star), feldspar (red, plus sign), montmorillonite (gray, pentagon) and natural desert and volcanic dust (green, square with cross). n_s datasets used in this figure were obtained from the studies listed in Table S2.

The n_s data were binned into 1 °C intervals at -38 < T < -2 °C and shown as boxplots in Figure S1. The median n_s values among different dust species differ by 1–6 orders of magnitude at identical temperatures (-38 < T < -18 °C), highlighting the influence of mineral composition on dust INA. Previous studies have reported that feldspar, particularly potassium-rich feldspar (K-feldspar), tends to exhibit higher INA compared to other dust species (Peckhaus et al., 2016; Atkinson et al., 2013; Augustin-Bauditz et al., 2014; Chen et al., 2023b; Harrison et al., 2016). Consistent with these findings, feldspars (plus signs in Figure 1 and red box in Figure S1) in the present study generally exhibit the highest n_s values at T ≤ -2 °C and initiated freezing at the warmest temperature (≈ -2 °C) compared to other dust species. For example, the extremely efficient dust particles at -20 < T < -5 °C and at T < -20 °C were from K-feldspar measured by Peckhaus et al. (2016) and Augustin-Bauditz *et al.* 2014[33], respectively. Some ATD (dark blue, triangle) (Kanji et al., 2013; Perkins et al., 2019) and natural volcanic dust (green, squares with cross) measured by Fahy et al. (2022) also display relatively high n_s values at warm freezing temperature (≈ -2 °C). Such high INA of ATD and volcanic dust was attributed

https://doi.org/10.5194/egusphere-2025-6368
Preprint. Discussion started: 18 February 2026

to the presence of K-feldspar in these particles, as supported by mineral and chemical characterizations of ATD (Chen et al., 2023b; Broadley et al., 2012) and volcanic dust (Fahy et al., 2022). The n_s boxplots of different dust species (Figure S1) show a similar trend, with K-feldspar exhibiting the highest INA followed by ATD. However, not all feldspars are as ice-active as K-feldspar. As shown in Figure 1 and Figure S1, non-potassium-rich feldspars can exhibit n_s values as low as those of quartz and illite (Harrison et al., 2016) at -21 < T < -5 °C. Similar variability of n_s is also observed for other dust species, including illite, ATD and quartz (Figure 1 and Figure S1). This variability can be partly explained by the inherent complexity of chemical composition, crystal structure and surface properties of dust, even for particles within the same mineral group. For example, several studies (Peckhaus et al., 2016; Harrison et al., 2016) found that K-feldspar exhibits higher INA than calcium-rich feldspars. The high INA of K-feldspar has been linked to surface defects with a particular crystallographic face (Kiselev et al., 2017) and to the kosmotropic (structure making) characteristic of K^+ in the surface layer (Zolles et al., 2015). Although Kumar et al. (2018) indicate that the high INA of K-feldspar may not be due to the presence of K^+, they observed decreased INA of K-feldspar when more K^+-containing solutes are added to dust suspensions. Harrison et al. (2019) measured the INA of 10 types of α-quartz samples and found that n_s varied 1–2 orders of magnitude at $T \approx$ -13 °C.

3.2 Impact of measurement methods on INA of dust particles and ice formation parameterization development

In addition to the compositional diversity of dust particles, the variability in n_s can also arise from differences in measurement methods, as suggested by Hiranuma et al. (2015) and Emersic et al. (2015). Accordingly, we divided the n_s values of each dust component into two groups: dry-dispersed aerosol (aerosol, hollow circles) and wet-suspended particles (suspension, solid circles) and shown in Figure 2. n_s values obtained from the two methods differ at identical temperatures. For example, aerosol n_s of feldspar (red) is 1–8 orders of magnitude higher than suspension n_s at T =-20 °C. Figure S2 presents boxplots of n_s separated by methods for different dust compositions (illite, ATD, K-feldspar, natural dust and kaolinite). The median n_s values between aerosol and suspension differ by 1–5 orders of magnitude at overlapping temperatures, with K-feldspar and kaolinite n_s showing the closest agreement between the two methods (Figure S2).

https://doi.org/10.5194/egusphere-2025-6368
Preprint. Discussion started: 18 February 2026

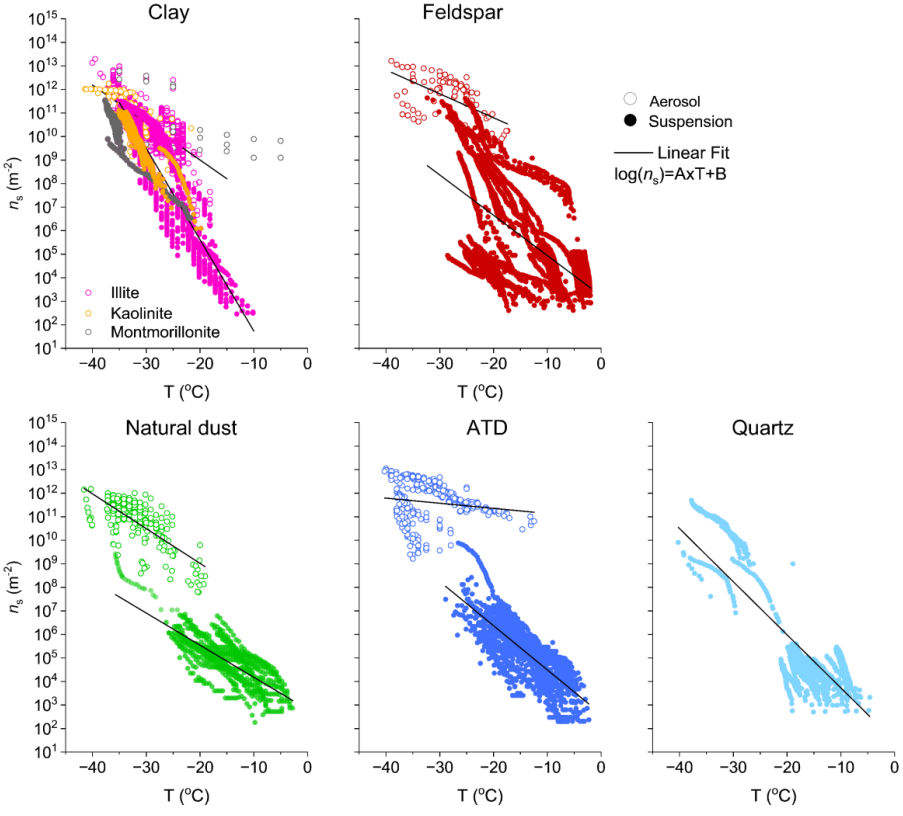

Figure 2. n_s of dust particles with specific mineral compositions. Clay particles comprise illite (pink), kaolinite (yellow), and montmorillonite (gray). Hollow and solid circles denote measurements using dry-dispersed aerosol and wet suspended particles, respectively. For quartz particles, only data from suspension measurements are available. Solid lines indicate linear fits of log (n_s) versus temperature, plotted separately for each measurement method. The values for fitting parameters (A and B) for each plot are listed in Table S3. The data used in this figure were obtained from the studies listed in Table S2.

Figure 3a compiles data from different compositions, showing that aerosol measurements (red) generally yield larger n_s values compared to suspension measurements (blue). The corresponding n_s boxplots for the combined data are shown in Figure S3a. The median values of aerosol n_s are 1–6 orders of magnitude higher than suspension n_s at -38 < T < -18 °C, with the n_s gap narrowing with decreasing temperatures. These findings confirm that measurement method is a large source of n_s variability and that the magnitude of this effect depends on dust composition. In addition, wet suspension n_s exhibits two distinct regimes of

https://doi.org/10.5194/egusphere-2025-6368
Preprint. Discussion started: 18 February 2026

increases (Figure 3a and Figure S3a), with a steeper temperature dependence observed at -38 < T < -18 °C compared to -18 < T < -3 °C.

To account for the time-dependent nature of ice nucleation, the J_{het} was estimated using Eq. (5) and Eq. (6) and shown in Figure 3b. The corresponding J_{het} boxplots are shown in Figure S3b. Similar to n_s, aerosol J_{het} values are systematically higher than suspension J_{het} values (Figure 3b), with differences in median J_{het} values up to 6 orders of magnitude at -37 < T < -19 °C (Figure 3Sb). The gap between aerosol and suspension J_{het} narrows with decreasing temperature and becomes comparable (within one order of magnitude) at T < -27 °C. Similar to n_s, suspension J_{het} also shows a stronger temperature dependence at -42 < T < -18 °C while remain relatively constant at T > -18 °C. The two-step temperature dependence of both n_s and J_{het} underscores the necessity of explicitly incorporating this feature into ice formation parameterizations. Neglecting this feature may lead to an underestimation of dust INA at colder temperatures (T < -18 °C) and overestimation of n_s and J_{het} at warmer temperatures (T > -18 °C).

The discrepancy between aerosol and suspension n_s and J_{het} may be attributed to differences in water-particle interactions between two methods (Emersic et al., 2015; Hiranuma et al., 2015). In DFTs (suspension), particles are suspended in water droplets prior to freezing measurements, whereas in chamber experiments (aerosol), particles activate into cloud droplets in situ within a few seconds. This different timescale of water-particle contact can cause varying degrees of particle surface alteration, thereby influencing their INA (Hiranuma et al., 2015). This process, known as water aging (Harrison et al., 2019; Kumar et al., 2019b), its impact on dust INA is further explored in section 3.3. Another important factor is the difference in particle concentrations within droplets generated by the two methods. Suspension samples in DFTs are typically prepared at higher particle concentrations, whereas chamber measurements detect freezing of droplets activated from individual particles. As noted by Emersic et al. (2015), high particle concentrations may cause coagulation either within suspensions or within the formed droplets, reducing the effective surface area available for nucleation and thereby lowering INA.

https://doi.org/10.5194/egusphere-2025-6368
Preprint. Discussion started: 18 February 2026

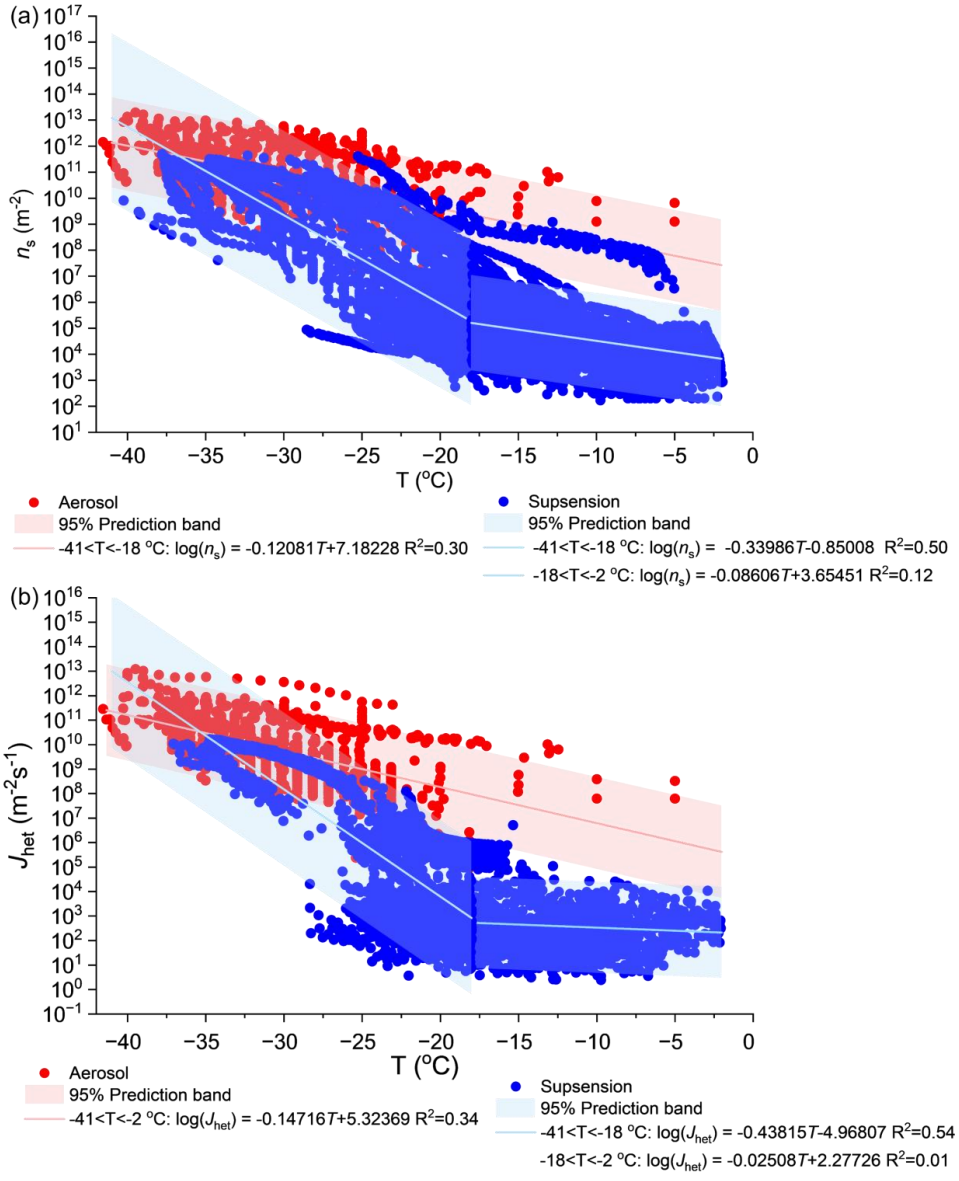

Figure 3. (a) n_s and (b) J_{het} of dust particles obtained from two measurement methods, dry-dispersed dust aerosol measured using ice nucleation chambers (aerosol, red) and wet-suspended particles measured using DFTs (suspension, blue). Solid lines are fitting curves of n_s or J_{het} versus temperatures, which are in the form: $\log(n_s \; or \; J_{het}) = A \times T + B$ (values for parameter A and B are listed in this figure).

https://doi.org/10.5194/egusphere-2025-6368
Preprint. Discussion started: 18 February 2026

To examine this coagulation effect, we calculated the spherical equivalent diameter (D_e) of dust particles contained in a droplet for both measurement methods. This calculation assumes the surface area available for ice nucleation in a droplet comes from a single INP, as is typically the case in the atmosphere. The surface area in the droplets, the S_p in aerosol measurement (Eq. (1)) and S_d in suspension measurement (Eq. (3)), is then used to calculate the diameter of the spherical equivalent particle ($D_e = \sqrt{\frac{S_p \text{ or } S_d}{\pi}}$). The relationship between D_e and droplet freezing temperatures (T) is shown in Figure 4, where the freezing temperature corresponds to the point at which 50% of droplets (FF = 50%) are frozen in the suspension measurements, and at which 10% of particles (AF = 10%) are ice-activated in the aerosol measurements. The freezing temperature of dust particles increases with D_e, and larger D_e values were obtained from suspension measurements than aerosol measurements at identical freezing temperatures (Figure 4a). For example, suspension D_e values are 1–3 orders of magnitude larger than those from aerosol measurements at T = -25 °C, indicating that the relatively warm temperature freezing (T > -25 °C) from suspension experiments would only be relevant for exceptionally large dust particles (≈ 10–7000 µm) in the atmosphere. Particles with different mineral compositions indicate a similar trend (Figure 4b), with larger suspension D_e values. This explains why suspension droplet experiments freeze at warmer temperatures than droplets activated from individual aerosol particles (Figure 4), as a greater particle surface area increases the probability of ice formation. However, such elevated particle concentrations in suspension measurements are also expected to enhance particle coagulation, which reduces the effective surface area available for ice nucleation and thereby decreases the freezing efficiency of suspension droplets. Since n_s is obtained by normalizing freezing ability of droplets with the suspension BET surface area, the calculated n_s are lower than those that would be obtained in the absence of coagulation (i.e., a case similar to aerosol measurement with individual particles).

https://doi.org/10.5194/egusphere-2025-6368
Preprint. Discussion started: 18 February 2026

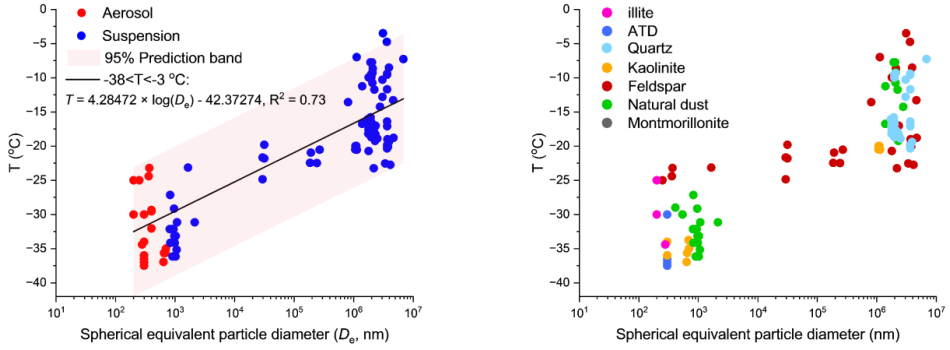

Figure 4. Spherical equivalent diameter (D_e) of dust particles in droplets derived from (a) aerosol (red) and suspension (blue) measurements, and (b) dust particles with different mineral compositions. The temperature shown in this figure represents the point at which 50% of droplets (FF=50%) are frozen in the suspension measurements, and at which 10% of particles (AF=10%) are ice activated in the aerosol measurements. D_e is calculated from studies in which S_p and S_d were provided or could be derived. The solid line is the fitting curve of freezing temperature versus $\log(D_e)$, which are in the form: $T = A \times \log(D_e) + B$ (values for parameter A and B are listed in this figure).

We also noted that there are few suspension D_e (≈ 1 μm) at -38 < T < -22 °C similar to that of aerosol measurements (Figure 4). These data correspond to suspension measurements with picoliter-size droplets, rather than from microliter-droplet measurements at warmer temperatures and therefore result in dust equivalent particle sizes (≈ 1 μm) that are more atmospherically relevant. Simulations by Emersic et al. (2015) suggest that picoliter-size droplets are unlikely to contain multiple particles to result in significant coagulation effects compared to microliter-sized droplets. Consequently, the freezing behavior of picoliter-size droplets is more comparable to droplets activated from single particles in aerosol measurements. This interpretation is also consistent with Figure 3 and Figure S3, where the n_s and J_{het} difference between two methods decreases with decreasing temperatures. This is because DFT measurements at relatively lower temperatures (-38 < T < -19 °C) were conducted using picoliter-size droplets (Table S2) (Atkinson et al., 2013; Hiranuma et al., 2015; Zolles et al., 2015) with negligible particle coagulation.

These findings suggest that coagulation effect may partly explain the different n_s values obtained between two methods, especially that observed for relatively warm temperatures. However, such coagulation-induced effects are primarily artifacts of the high particle

https://doi.org/10.5194/egusphere-2025-6368
Preprint. Discussion started: 18 February 2026

concentrations used in laboratory suspensions and are unlikely to occur under typical atmospheric conditions, where individual cloud droplets generally contain only a single dust particle. As a result, n_s values obtained from aerosol measurements with individual particles are more representative of fresh dust particles emitted near the source, where particles remain largely unaggregated and have minimal interactions with water in arid environments. While suspension n_s are unlikely to be relevant for dust particle freezing in the atmosphere regarding coagulation, they may reflect the INA of particles subjected to water-aging processes, which will be discussed in section 3.3. If ice formation parameterizations are developed based on suspension n_s, they will likely underestimate the INA of dry and fresh dust aerosol particles. Overall, the different n_s obtained from the two methods highlight the need to develop parameterizations that account for these distinctions.

Based on the findings in this section and section 3.1, we fitted the n_s and J_{het} temperature dependent parameterizations using a log-linear form:

$$\log(n_s) = A \times T + B$$

The fitted parameters (A, B) and coefficients of determination (R^2) for different measurement methods are indicated in Figure 3 and summarized in Table S3. For example, aerosol n_s shows a weak correlation with temperatures at -41 < T < -13 °C, expressed as follows. To represent the INA of dust aerosol across the entire MPC temperature range, this fitted relationship was extrapolated to T = -2 °C (Figure 3a). This aerosol n_s parameterization represents the INA of dry and near-source dust aerosol that have a negligible effect from water exposure:

$$\log(n_s) = -0.12081T + 7.18228\ (R^2 = 0.30)$$

As discussed above, suspension n_s exhibits two-step temperature dependence, with a stronger temperature dependence at -41 < T < -18 °C and a weaker dependence at -18 < T < -2 °C. Accordingly, the suspension n_s data were fitted separately in two temperature regimes. The resulting parameterizations are summarized below:

-41 < T < -18 °C:

$$\log(n_s) = -0.33986T - 0.85008\ (R^2 = 0.50)$$

-18 < T < -2 °C:

$$\log(n_s) = -0.08606 + 3.65451\ (R^2 = 0.12)$$

https://doi.org/10.5194/egusphere-2025-6368
Preprint. Discussion started: 18 February 2026

The prediction band at the 95% confidence level (shaded area in Figure 3) captures most data points (Figure 3a), indicating the strong predictive capability of the developed n_s parameterizations. Specifically, 4449 out of 4661 and 5062 out of 5321 n_s values for suspension measurements at T < -18 °C and T > -18 °C were captured, and 1462 out of 1535 for aerosol measurements were captured. Similar parameterizations were developed for J_{het} with the resulting functions shown in Figure 3b.

Given the distinct INA among dust particles with different compositions, we also developed n_s parameterizations for individual dust species, as indicated by the log-linear fits in Figure 2 and summarized in Table S3. These composition-specific parameterizations (Figure 2 and Table S3) are intended for estimating atmospheric INP contributions from individual mineral types. They are therefore suitable in regions where a single mineral dominates the dust population, if its local abundances are known. In contrast, the parameterizations developed from the dataset of all dust types (Figure 3) represent the average freezing behavior of dust particles with mixed mineral compositions, which are suitable for predicting INPs in an atmosphere with compositionally diverse dust or for global-average applications.

As mentioned above, suspension-derived n_s often involves measurements using unrealistically high particle concentrations that promote artificial coagulation, which is unlikely to occur in real-world cloud droplets containing only one particle. In addition, applying n_s-based parameterizations for aerosol and suspension requires distinguishing whether dust particles have been influenced by water exposure, necessitating additional physicochemical characterization of particle surfaces. To address these limitations, an D_e-based parameterization was developed by fitting D_e as a function of droplet freezing temperature:

-38 < T < -3 °C:

$$T = 4.28472 \times \log(D_e) - 42.37274 \ (R^2 = 0.73)$$

As shown in Figure 4a, this D_e parameterization is independent of measurement method and predicts the freezing temperature of droplets directly from the surface area of immersed particles. It is applicable across the MPC temperature regime and can be readily used whenever particle size information is available. The 95% prediction band (shaded area in Figure 4) demonstrates the strong predictive capability of the developed D_e parameterization, with 120 out of 122 data points successfully captured.

https://doi.org/10.5194/egusphere-2025-6368
Preprint. Discussion started: 18 February 2026

3.3 n_s of dust particles subjected to different aging processes

The INA changes resulting from various aging processes are also investigated. Experimental details of aging treatments are provided in Table S2. Figure 5 shows n_s data for fresh (solid colors) and aged (faded colors) dust particles, with dry aerosol (Figure 5a) and wet suspension (Figure 5b) shown separately. For both aerosol and suspension, fresh (solid colors) and aged particles (faded colors) exhibit differences in n_s at identical temperatures. This indicates that atmospheric aging modifies the INA of dust particles. To quantify these differences, n_s data were binned into 1 ℃ intervals and are shown in Figure S4. For aerosol measurements (Figure S4a), the median n_s values of fresh (solid color) and aged (faded color) particles differ by 1–2 orders of magnitude at -41 < T < -20 ℃. A similar difference is observed in fresh and aged suspension n_s at -27 < T < -3 ℃ (Figure S4b). These differences are notably smaller than those caused by measurement methods. For example, the discrepancy between n_s from dry-dispersion and wet-suspension can reach 1–6 orders of magnitude in the same temperature range (Figure 3 and Figure S3). In addition, n_s of both fresh and aged particles from suspension measurements (Figure S4b) exhibit a stronger temperature dependence at lower temperature (-38 < T < -18 ℃) and a weaker dependence at higher temperature (-18 < T < -3 ℃). This feature aligns with the observation when fresh and aged datasets are combined (Figure S3). Therefore, n_s parameterizations for fresh and aged particles are developed by explicitly considering their temperature dependence, as shown in Figure 5. For both fresh and aged aerosol measurements, the n_s parameterizations are extrapolated to T = -2 ℃ (Figure 5a) to represent the INA of dust particles to represent the ice-nucleating activity (INA) of dust particles that have experienced minimal interaction with water across the entire MPC temperature range.

https://doi.org/10.5194/egusphere-2025-6368
Preprint. Discussion started: 18 February 2026

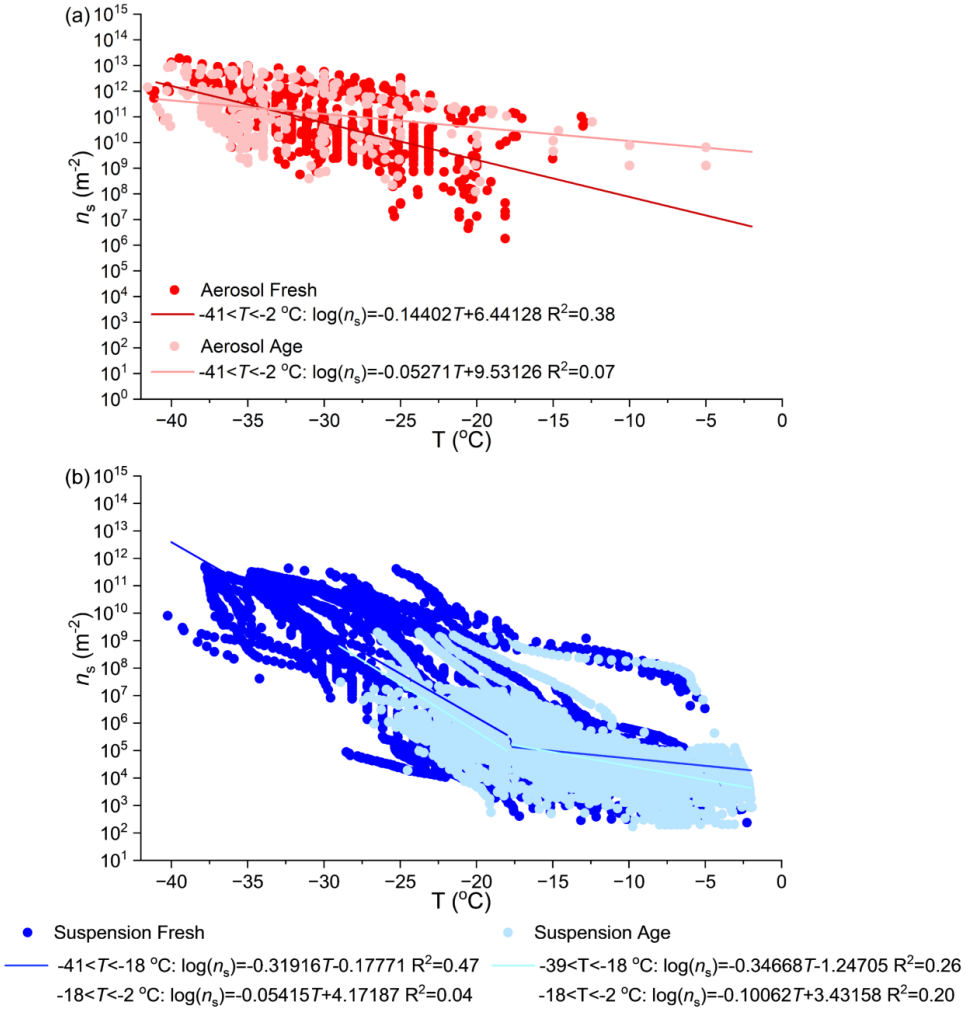

Figure 5. n_s of dust particles measured freshly (solid colors) and after aging treatments (faded colors) from (a) aerosol and (b) suspension methods. The parameterizations to predict n_s of dust particles are of the form: $log(n_s) = A \times T + B$ (values for parameter A and B are listed in this figure and Table S3). For n_s from suspension measurements, parameterizations are developed in two different temperature regimes (T < -18 °C and T > -18 °C), respectively. The data used in this figure was obtained from the studies listed in Table S2.

Based on Figure 5 and Figure S4, it is challenging to draw a conclusion on how the aging process will impact the INA of dust particles, since aging does not consistently increase or decrease n_s at different temperatures. The direction and magnitude of the aging effect may depend on the specific dust species and the aging pathways. To account for this, Figure S5

https://doi.org/10.5194/egusphere-2025-6368
Preprint. Discussion started: 18 February 2026

provides elaborated n_s boxplots for individual dust species, including K-feldspar, non-potassium-rich feldspars, quartz, ATD and natural dust. Clay particles are not shown due to limited data from two methods for comparison between fresh and aged particles. Given the significant contribution of clay particles to dust mass (Atkinson et al., 2013), additional measurements are needed to quantify the aging effect on their INA. Figure S5 indicates that aging may have different effects on INA of different dust species. Specifically, ATD and natural dust show a decrease of 1–2 orders of magnitude in n_s at -39 < T < -3 °C after aging, with the effect becoming more pronounced at lower temperatures. In contrast, the n_s changes of K-feldspar and quartz particles are generally within one order of magnitude, indicating that these dust species are relatively insensitive to aging. This observation is consistent with Harrison et al. (2016), who found most K-feldspars exhibited no significant change in INA after water aging. While Harrison et al. (2019) noted that certain quartz can be highly sensitive to water aging, only one of the three samples exhibited a pronounced decrease in n_s after 10 months of water aging, whereas n_s decrease of other quartz samples were within one order of magnitude. Their findings therefore align with our results showing insensitive of quartz to aging treatments. The response of non-potassium-rich feldspar ("other feldspars" in Figure S5) (Harrison et al., 2019; Peckhaus et al., 2016) to aging process, including albite and anorthite, is more variable. Depending on temperature, aging can increase, decrease or leave their n_s unchanged (Figure S3). For most temperatures, the n_s changes of other feldspars remain within one order of magnitude. An exception occurs at -25 < T < -23 °C, where the n_s of aged particles increased by 2–5 orders of magnitude compared to fresh particles. This occurs because most fresh non-potassium-rich feldspars exhibit relatively low INA. However, one aged sample from Harrison et al. (2016) displayed markedly higher INA, which strongly influenced the median n_s values. This variability reflects both the compositional diversity of feldspars and the limited number of available datasets for aged non-potassium-rich feldspars, as indicated in Figure S5. Overall, our results suggest that feldspars (both K-feldspar and other feldspars) and quartz are generally insensitive to aging process compared to natural dust and ATD.

We further investigate how different aging pathways influence the dust INA and develop corresponding n_s parameterizations. As mentioned in the methodology, laboratory aging treatments (Table S2) are categorized into four groups: water aging, aqueous aging (salt and acid solutions), gas chemical and coating, and thermal treatments. The resulting n_s boxplots of dust particles subjected to these aging processes are presented in Figure 6. It should be noted

https://doi.org/10.5194/egusphere-2025-6368
Preprint. Discussion started: 18 February 2026

that only studies reported paired measurements of fresh and aged n_s for the same dust type are considered. This restriction is necessary because n_s values vary strongly among mineral species, and some species may have measurements only for the fresh state. Including such incomplete datasets could bias the median n_s of fresh dust. For example, if the relatively low n_s of fresh quartz (Figure 1) was included and compared to aged feldspar n_s with exceptionally high INA (Figure 1), the overall median n_s for fresh dust would be artificially lowered, confounding the assessment of aging effects. A similar artifact was observed in the case of non-potassium-rich feldspars (Figure S5) at -25 < T < -23 °C, where the median n_s of aged particles appears higher than fresh particles, due to the inclusion of datasets lacking paired measurements. For reference, the n_s derived from the complete datasets (without this restriction) is presented in Figure S6. As expected, n_s values of fresh dust overlap with those from different aging processes, making it difficult to isolate the impact of each aging process (Figure S6). This is because the larger number of the fresh n_s datasets compared to aged n_s and their strong variability caused by mineral compositions. To minimize this bias, we therefore focus on paired datasets of fresh and aged n_s and develop parameterizations accordingly (Figure 6).

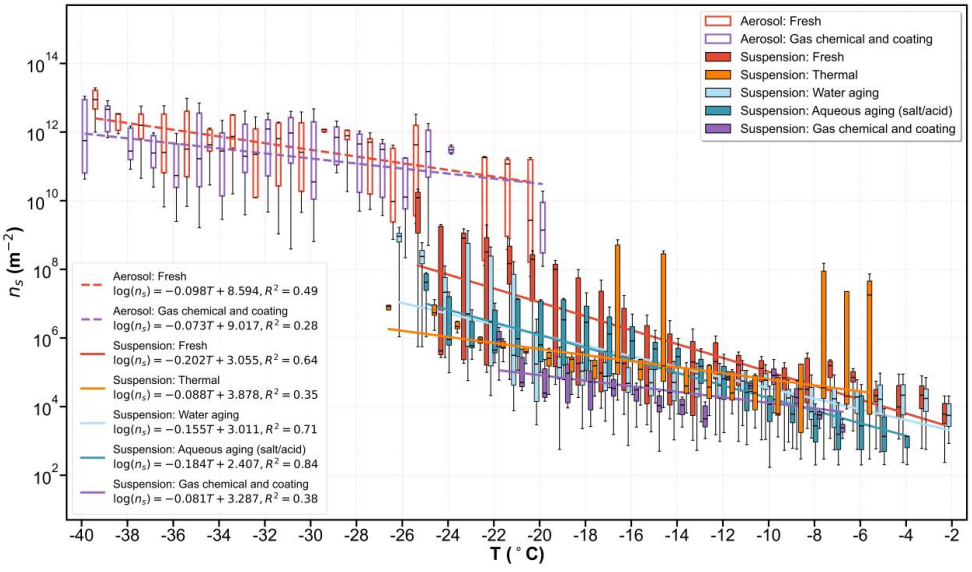

Figure 6. n_s of dust particles measured freshly (red) and after being subjected to different aging processes, including water aging (light blue), aqueous aging (dark blue), thermal treatment (orange), gas chemical reactions and coating (purple). The datasets obtained from dry-dispersed aerosol (open box) and wet-suspended particles (solid box) are shown separately. Only n_s data

https://doi.org/10.5194/egusphere-2025-6368
Preprint. Discussion started: 18 February 2026

from selected studies is presented, including results obtained from feldspar, quartz, ATD and natural dust, in which both fresh and aged dust particles of the same type were measured (more details in Table S2). The parameterizations to predict n_s of dust particles aged through different processes are of the form: $log(n_s) = A \times T + B$.

As shown in Figure 6, both aerosol (open box) and suspension (solid box) aging exert variable impacts on the INA of dust particles at -40 < T < -2 °C. The aerosol and suspension n_s across different aging processes vary by 1–2 and 1–4 orders of magnitude at -40 < T < -20 °C and -26 < T < -2 °C, respectively. By fitting the median n_s values at different temperatures, we find that aged particles (both aerosol and suspension) generally exhibit lower INA than fresh particles (red curves). This aligns with most studies (Table S2), which report reduced INA after various aging treatments. The only exceptions are montmorillonite (Salam et al., 2007) and K-feldspar (Kumar et al., 2018), which showed increased INA after exposure to NH_3 gas and NH_4^+ solutions. The fitting curves in Figure 6 therefore represent the average INA of fresh and aged dust particles with mixed mineral compositions which is representative of atmospheric dust populations.

For suspension measurements, aging via chemical reactions and coating causes the most significant decrease in dust INA (purple curves), followed by thermal treatment (orange curves). Aqueous aging of dust particles in water (light blue curves) or salt/acid solutions (dark blue curves) also decreases INA of dust particles. The impacts from these two pathways are similar but weaker than those induced by chemical and thermal treatment. This trend is also supported by a case study of ATD, the only dust species for which INA has been reported under all aging treatments. Figure S7 explicitly shows the n_s boxplots of fresh and aged ATD. Specifically, suspension measurements of ATD show the largest decrease in n_s under gas chemical and coating aging, followed by thermal treatment. The impact of water and aqueous aging are similar but less significant compared to the other two aging processes. The results from ATD confirm that the general conclusion drawn from selective studies (Figure 6) is representative of the aging impact on individual dust species. Given the different magnitudes of aging effects, we developed separate n_s parameterizations for dust particles subjected to distinct aging processes, as listed in Figure 6. However, to represent the INA of bulk fresh and aged particles, we would recommend using parameterizations listed in Figure 5, which better capture the average INA of dust particles with diverse compositions. We note that data for water and aqueous aging of dry-dispersed dust particles (aerosol) are very limited. This makes the evaluation of water and aqueous aging impact on dust particles from dry dispersion not feasible,

https://doi.org/10.5194/egusphere-2025-6368
Preprint. Discussion started: 18 February 2026

we thereby encourage further studies on this aspect. Nevertheless, the finding that water/aqueous aging generally reduces dust INA, may help explain the discrepancy in n_s between dust particles generated by dry dispersion and wet suspension (section 3.2). Because dust particles in suspensions remain in contact with water for longer periods during sample preparation, they are expected to exhibit lower n_s values relative to dry dispersed particles. We therefore emphasize that water should be considered a reactive medium in ice nucleation studies. In particular, the preparation and storage duration of dust suspensions may introduce uncertainties in quantifying the INA of dust particles and should be carefully controlled. It should also be noted that water aging only reduce dust n_s by 2 orders of magnitude at -26 < T < -2 °C, which is smaller than the n_s discrepancy observed between aerosol and suspension measurements within the same temperature range (up to 6 orders of magnitude at -26< T < -20 °C). This suggests that water aging alone cannot fully explain the n_s discrepancy caused by measurement method, the artificial coagulation effect (section 3.2) may be an important contributing factor.

4 Conclusions

In this study, we systematically revisited the INA of dust particles under mixed-phase cloud conditions using a comprehensive dataset compiled from previous laboratory measurements. We assessed the impact of mineral composition, measurement methods and various aging processes on the INA of dust particles, represented by n_s. Our results indicate that n_s of dust particles exhibit substantial variability across the studied temperature range (-42 < T < -2 °C), for example at T = -20 °C, n_s spans from 5.0×10^{3} to 9.0×10^{10} m^{-2}. Such significant variability can partly be attributed to the compositional diversity of dust particles. K-feldspar rich particles can trigger immersion freezing at the warmest temperature (≈ -2 °C) compared to other dust species with the same surface area (equivalent to particle sizes of 10^{7} nm), including clay and quartz particles. Even within a single mineral group, n_s varies significantly, for example, n_s of K-feldspar is 1–6 orders of magnitude higher than that of non-potassium-rich feldspar at -37 < T < -4 °C.

Measurement methods exert a systematic influence on dust n_s. Dry-dispersed particles generally demonstrate higher n_s than those produced from wet suspensions, with discrepancies of 1–6 orders of magnitude at -38 < T < -18 °C. This method-related difference likely arises from particle-water interactions occurring within droplets or suspensions, including particle coagulation and surface modification induced by water exposure. Compared with dry-dispersed

https://doi.org/10.5194/egusphere-2025-6368
Preprint. Discussion started: 18 February 2026

particles, suspension droplets with artificially high particle concentration undergo stronger particle coagulation, which reduces the effective surface area available for ice nucleation. In addition, particles experience longer water-contact time in suspension measurements, which may modify their surfaces and thereby reducing their INA. The difference between aerosol and suspension methods has been systematically shown for illite NX before (Hiranuma et al., 2015), but here we extend this analysis to other dust species including ATD, quartz, kaolinite, feldspar montmorillonite and natural dust.

By accounting for the variability in dust INA caused by mineral composition and measurement methods, we developed n_s-based parameterizations to predict INP numbers contributed by dust. Two types of parameterizations were established: those based on n_s of dust across mineral compositions, representing the average INA of dust particles; and those based on composition-specific n_s, reflecting the INA of dust with specific mineral compositions. All parameterizations are expressed in log-linear form: $\log(n_s) = A \times T + B$, with separate fits for dry and wet measurements. Suspension-derived n_s exhibits a two-regime temperature dependence, characterized by a steeper increase at T < -18 °C and a weaker increase at -18 < T < -2 °C. We developed segmented parameterizations that explicitly represent these two temperature regimes, thereby improving the prediction of dust INPs under different temperature conditions. Moreover, we developed a parameterization based on the spherical equivalent particle size within a droplet (D_e), by assuming the surface area available for ice nucleation in a droplet comes from a single INP. This D_e based parameterization predicts immersion freezing temperature of dust particles in a log-linear form at -38 < T < -3 °C: $T = A \times \log(D_e) + B$. Unlike the n_s parameterizations, it does not require distinguishing between measurement methods and temperature regimes, allowing for representing droplet freezing over the entire MPC temperature range with a single expression.

We also investigated the impact of atmospheric aging on dust INA. The aging processes studied include water and aqueous aging with salt or acid solutions, thermal treatment, and chemical aging through exposure to reactive gases or coating with inorganic or organic aerosol. Our results indicate that aging modifies dust INA in composition- and process- specific ways. While n_s of most dust particles reduced after aging by 1−4 orders of magnitude at -40 < T < -2 °C, K-feldspar and quartz exhibit limited sensitivity to aging treatments. Among aging treatments, chemical reactions with gas or coating with organic/inorganic compounds induce the strongest reduction in dust INA, followed by thermal treatments. Water and aqueous aging

https://doi.org/10.5194/egusphere-2025-6368
Preprint. Discussion started: 18 February 2026

produce a similar but smaller reduction in dust n_s (2 orders of magnitude at -26 < T < -2 °C) compared to other treatments. This finding confirms that water can act as a reactive medium that alters the ice nucleation of dust particles. However, the reduction in n_s caused by water/aqueous aging alone cannot account for the discrepancy in n_s observed for different measurement methods (up to 6 orders of magnitude at -26 < T < -20 °C), indicating that the artificial coagulation effect has a greater effect on the determined dust INA. Based on these results, we developed aging process-specific n_s parameterizations to represent the INA of aged particles.

5 Atmospheric implications

All n_s-based parameterizations can be applied to estimate the contribution of dust aerosol to INP concentrations and primary ice formation in different atmospheric scenarios, if the corresponding surface area of dust particles is known. The parameterizations that represent the average freezing ability of dust particles are appropriate for atmospheres with compositionally diverse dust or for global-average applications. The composition-specific parameterizations are tailored to conditions where the INP population is largely governed by a single mineral type, making them more suitable for regional or local applications.

Wet-suspended dust particles generally exhibit lower INA (n_s) than dry-dispersed aerosol, due to water-mediated processes. Therefore, n_s parameterizations derived from dry-dispersed aerosol are most representative of freshly emitted, dry dust near source regions, while those derived from suspension measurements are more relevant to particles that have undergone water-induced changes like being transported in cloudy conditions where the particles are subjected to CCN activated trajectories. However, suspension n_s measurements at warmer temperature often use unrealistically high particle concentrations, which can promote artificial particle coagulation and artificially reduce the measured dust INA. Consequently, applying aerosol and suspension n_s -based parameterizations to atmospheric conditions requires additional information on water-particle interactions (e.g., particle concentration, solutes and interaction time) and further physicochemical characterizations of dust particles. D_e-based parameterizations overcome these limitations by linking immersion freezing temperatures of dust particles directly to particle size even when details of particle-water interactions are unknown. This approach is independent of measurement methods and allows prediction of dust freezing without the need to consider complex water or aging trajectories in models. In addition, n_s is derived by assuming that the distribution and properties of active sites do not change with

https://doi.org/10.5194/egusphere-2025-6368
Preprint. Discussion started: 18 February 2026

particle size. This assumption introduces uncertainties in dust INA, because atmospheric dust tends to be polydisperse and exhibits size-dependent variations in mineral composition and surface structure that may alter its freezing activity. In contrast, D_e-based parameterizations account for size-dependent variations in droplet freezing behavior by assigning freezing temperatures of droplets according to particle size. In suspension measurements, the reduced dust INA due to water aging also highlights the importance of controlling the particle-water contact during the preparation, storage, and measurement of dust suspensions. Atmospherically relevant particle concentrations should be used in suspension experiments to avoid artificial coagulation that alter dust INA.

Similar to water aging, chemical reactions and thermal processes also reduce dust INA, though to different extents. The aging process-specific n_s parameterizations developed here therefore provide a more realistic representation of INA for aged dust particles. When applying these parameterizations in climate models, it is important to consider the atmospheric history of dust plumes. For example, dust transported through regions with severe air pollution is better represented by parameterizations for chemically aged particles, whereas dust plumes that remain over oceans for extended periods may be better represented by parameterizations for water- or aqueous- aged particles.

Overall, this study provides physically grounded parameterizations for representing dust INA under MPC conditions. Nevertheless, several limitations remain and further studies are warranted. INP data for dry-dispersed dust aerosol of different compositions, such as clay and quartz particles are still limited, introducing uncertainties in developing composition-specific and aerosol-derived n_s parameterizations. The aging process-specific parameterizations developed here are based solely on suspension measurements, as comparative experiments on fresh and aqueous-aged of dry-dispersed dust particles are scarce. In addition, these aging parameterizations do not account for the time scale of aging. Future studies should systematically investigate time-dependent aging to improve INP predictions across different stages of dust plume evolution. To further evaluate the developed parameterizations, INP concentrations predicted by n_s-based and D_e-based parameterizations should be inter-compared, to those from existing INP parameterizations, and to field observations influenced by dust emissions. This will be addressed in a separate study. These comparisons will aid in quantifying the differences in estimated ice production when different parameterizations are applied, and evaluate biases compared to observed atmospheric INP

https://doi.org/10.5194/egusphere-2025-6368
Preprint. Discussion started: 18 February 2026

concentrations. For implementation of aging-specific parameterizations in climate models, it is important to distinguish and represent fresh and aged dust particles subjected to different aging processes within the aerosol emission schemes, and to integrate this information with the developed parameterizations to better estimate primary ice formation induced by dust under diverse atmospheric scenarios.

Author contributions

J.C collected INP datasets from available resources. J.C and Z.A.K developed dust ice formation parameterizations and completed the manuscript.

Competing interests

All authors declare no competing interests.

Data availability

The data used in this work will be made available through a persistent DOI upon acceptance of the manuscript.

Acknowledgments

All datasets used in this work are published and were compiled from digitized figures in the literature, open-access repositories, or data provided directly by corresponding authors. We specifically acknowledge the following researchers for sharing their INP data: Dr. Alexei Kiselev (Karlsruhe Institute of Technology), Prof. Benjamin Murray (University of Leeds), Dr. Heike Wex (Leibniz Institute for Tropospheric Research), Dr. Gourihar Kulkarni (Pacific Northwest National Laboratory), Prof. Naruki Hiranuma (West Texas A&M University), Dr. Russell J. Perkins (Colorado State University), and Dr. Xiadi Lan Chen (Guangzhou Institute of Geochemistry).

Financial support

This project has received funding from Horizon Europe Programme under Grant Agreement No. 101137680 via project CERTAINTY (Cloud-aERosol inTeractions & their impActs IN The earth sYstem).

Reference

Ansmann, A., Tesche, M., Althausen, D., Müller, D., Seifert, P., Freudenthaler, V., Heese, B., Wiegner, M., Pisani, G., Knippertz, P., and Dubovik, O.: Influence of Saharan dust on cloud glaciation in southern Morocco during the Saharan Mineral Dust Experiment, Journal of Geophysical Research: Atmospheres, 113, https://doi.org/10.1029/2007JD008785, 2008.

Atkinson, J. D., Murray, B. J., Woodhouse, M. T., Whale, T. F., Baustian, K. J., Carslaw, K. S., Dobbie, S., O'sullivan, D., and Malkin, T. L.: The importance of feldspar for ice nucleation by mineral dust in mixed-phase clouds, Nature, 498, 355, https://doi.org/10.1038/nature12278, 2013.

https://doi.org/10.5194/egusphere-2025-6368
Preprint. Discussion started: 18 February 2026

699 Augustin-Bauditz, S., Wex, H., Kanter, S., Ebert, M., Niedermeier, D., Stolz, F., Prager, A., and
700 Stratmann, F.: The immersion mode ice nucleation behavior of mineral dusts: A comparison of
701 different pure and surface modified dusts, Geophysical Research Letters, 41, 7375–7382,
702 https://doi.org/10.1002/2014GL061317, 2014.

703 Boose, Y., Welti, A., Atkinson, J., Ramelli, F., Danielczok, A., Bingemer, H. G., Ploetze, M.,
704 Sierau, B., Kanji, Z. A., and Lohmann, U.: Heterogeneous ice nucleation on dust particles
705 sourced from nine deserts worldwide-Part 1: Immersion freezing, Atmospheric Chemistry and
706 Physics, 16, https://doi.org/10.5194/acp-16-15075-2016, 2016.

707 Broadley, S. L., Murray, B. J., Herbert, R. J., Atkinson, J. D., Dobbie, S., Malkin, T. L.,
708 Condliffe, E., and Neve, L.: Immersion mode heterogeneous ice nucleation by an illite rich
709 powder representative of atmospheric mineral dust, Atmospheric Chemistry and Physics, 12,
710 287–307, https://doi.org/10.5194/acp-12-287-2012, 2012.

711 Budke, C. and Koop, T.: BINARY: an optical freezing array for assessing temperature and time
712 dependence of heterogeneous ice nucleation, Atmospheric Measurement Techniques, 8, 689–
713 703, https://doi.org/10.5194/amt-8-689-2015 2015.

714 Burrows, S. M., McCluskey, C. S., Cornwell, G., Steinke, I., Zhang, K., Zhao, B., Zawadowicz,
715 M., Raman, A., Kulkarni, G., China, S., Zelenyuk, A., and DeMott, P. J.: Ice-Nucleating
716 Particles That Impact Clouds and Climate: Observational and Modeling Research Needs,
717 Reviews of Geophysics, 60, e2021RG000745, https://doi.org/10.1029/2021RG000745, 2022.

718 Chen, J., Wu, Z., Gong, X., Qiu, Y., Chen, S., Zeng, L., and Hu, M.: Anthropogenic Dust as a
719 Significant Source of Ice-Nucleating Particles in the Urban Environment, Earth's Future, 12,
720 e2023EF003738, https://doi.org/10.1029/2023EF003738, 2024.

721 Chen, J. P., Hazra, A., and Levin, Z.: Parameterizing ice nucleation rates using contact angle
722 and activation energy derived from laboratory data, Atmospheric Chemistry and Physics, 8,
723 7431–7449, https://doi.org/10.5194/acp-8-7431-2008, 2008.

724 Chen, L., Worthy, S. E., Gu, W., Bertram, A. K., and Tang, M.: The Effects of Aminium and
725 Ammonium Cations on the Ice Nucleation Activity of K-Feldspar, Journal of Geophysical
726 Research: Atmospheres, 128, e2023JD039971, https://doi.org/10.1029/2023JD039971, 2023a.

727 Chen, L., Peng, C., Chen, J., Chen, J., Gu, W., Jia, X., Wu, Z., Wang, Q., and Tang, M.: Effects
728 of heterogeneous reaction with NO2 on ice nucleation activities of feldspar and Arizona Test
729 Dust, Journal of Environmental Sciences, 127, 210–221,
730 https://doi.org/10.1016/j.jes.2022.04.034, 2023b.

731 de Boer, G., Morrison, H., Shupe, M. D., and Hildner, R.: Evidence of liquid dependent ice
732 nucleation in high-latitude stratiform clouds from surface remote sensors, Geophysical
733 Research Letters, 38, https://doi.org/10.1029/2010GL046016, 2011.

734 DeMott, P. J., Prenni, A. J., Liu, X., Kreidenweis, S. M., Petters, M. D., Twohy, C. H.,
735 Richardson, M. S., Eidhammer, T., and Rogers, D. C.: Predicting global atmospheric ice nuclei
736 distributions and their impacts on climate, Proc. Natl. Acad. Sci. USA., 107, 11217–11222,
737 https://doi.org/10.1073/pnas.0910818107, 2010.

https://doi.org/10.5194/egusphere-2025-6368
Preprint. Discussion started: 18 February 2026

738 DeMott, P. J., Möhler, O., Cziczo, D. J., Hiranuma, N., Petters, M. D., Petters, S. S., Belosi, F.,
739 Bingemer, H. G., Brooks, S. D., and Budke, C.: The Fifth InternationalWorkshop on Ice
740 Nucleation phase 2 (FIN-02): laboratory intercomparison of ice nucleation measurements,
741 Atmospheric Measurement Techniques, 11, 6231–6257, https://doi.org/10.5194/amt-2018-191,
742 2018.

743 DeMott, P. J., Prenni, A. J., McMeeking, G. R., Sullivan, R. C., Petters, M. D., Tobo, Y.,
744 Niemand, M., Möhler, O., Snider, J. R., Wang, Z., and Kreidenweis, S. M.: Integrating
745 laboratory and field data to quantify the immersion freezing ice nucleation activity of mineral
746 dust particles, Atmospheric Chemistry and Physics, 15, 393–409, https://doi.org/10.5194/acp-
747 15-393-2015, 2015.

748 Emersic, C., Connolly, P. J., Boult, S., Campana, M., and Li, Z.: Investigating the discrepancy
749 between wet-suspension- and dry-dispersion-derived ice nucleation efficiency of mineral
750 particles, Atmospheric Chemistry and Physics, 15, 11311–11326, https://doi.org/10.5194/acp-
751 15-11311-2015, 2015.

752 Fahy, W. D., Maters, E. C., Giese Miranda, R., Adams, M. P., Jahn, L. G., Sullivan, R. C., and
753 Murray, B. J.: Volcanic ash ice nucleation activity is variably reduced by aging in water and
754 sulfuric acid: the effects of leaching, dissolution, and precipitation, Environmental Science:
755 Atmospheres, 2, 85–99, https://doi.org/10.1039/D1EA00071C, 2022.

756 Harrison, A. D., Lever, K., Sanchez-Marroquin, A., Holden, M. A., Whale, T. F., Tarn, M. D.,
757 McQuaid, J. B., and Murray, B. J.: The ice-nucleating ability of quartz immersed in water and
758 its atmospheric importance compared to K-feldspar, Atmospheric Chemistry and Physics, 19,
759 11343–11361, https://doi.org/10.5194/acp-19-11343-2019, 2019.

760 Harrison, A. D., Whale, T. F., Carpenter, M. A., Holden, M. A., Neve, L., apos, Sullivan, D.,
761 Vergara Temprado, J., and Murray, B. J.: Not all feldspars are equal: a survey of ice nucleating
762 properties across the feldspar group of minerals, Atmospheric Chemistry and Physics, 16,
763 10927–10940, https://doi.org/10.5194/acp-16-10927-2016, 2016.

764 Hiranuma, N., Augustin-Bauditz, S., Bingemer, H., Budke, C., Curtius, J., Danielczok, A.,
765 Diehl, K., Dreischmeier, K., Ebert, M., Frank, F., Hoffmann, N., Kandler, K., Kiselev, A., Koop,
766 T., Leisner, T., Möhler, O., Nillius, B., Peckhaus, A., Rose, D., Weinbruch, S., Wex, H., Boose,
767 Y., DeMott, P. J., Hader, J. D., Hill, T. C. J., Kanji, Z. A., Kulkarni, G., Levin, E. J. T.,
768 McCluskey, C. S., Murakami, M., Murray, B. J., Niedermeier, D., Petters, M. D., O'Sullivan,
769 D., Saito, A., Schill, G. P., Tajiri, T., Tolbert, M. A., Welti, A., Whale, T. F., Wright, T. P., and
770 Yamashita, K.: A comprehensive laboratory study on the immersion freezing behavior of illite
771 NX particles: a comparison of 17 ice nucleation measurement techniques, Atmospheric
772 Chemistry and Physics, 15, 2489–2518, https://doi.org/10.5194/acp-15-2489-2015, 2015.

773 Hoose, C. and Möhler, O.: Heterogeneous ice nucleation on atmospheric aerosols: a review of
774 results from laboratory experiments, Atmospheric Chemistry and Physics, 12, 9817–9854,
775 https://doi.org/10.5194/acp-12-9817-2012, 2012.

776 Huang, S., Hu, W., Chen, J., Wu, Z., Zhang, D., and Fu, P.: Overview of biological ice
777 nucleating particles in the atmosphere, Environment International, 146, 106197,
778 https://doi.org/10.1016/j.envint.2020.106197, 2021.

https://doi.org/10.5194/egusphere-2025-6368
Preprint. Discussion started: 18 February 2026

779 Huang, Z., Hu, W., Chen, J., Zhu, J., Wu, Z., Zhang, Y., and Fu, P.: Atmospheric aging effects
780 on aerosol ice nucleation, Earth-Science Reviews, 269, 105176,
781 https://doi.org/10.1016/j.earscirev.2025.105176, 2025.

782 Kanji, Z. A., Welti, A., Chou, C., Stetzer, O., and Lohmann, U.: Laboratory studies of immersion
783 and deposition mode ice nucleation of ozone aged mineral dust particles, Atmospheric
784 Chemistry and Physics, 13, 9097–9118, https://doi.org/10.5194/acp-13-9097-2013, 2013.

785 Kanji, Z. A., Ladino, L. A., Wex, H., Boose, Y., Burkert-Kohn, M., Cziczo, D. J., and Krämer,
786 M.: Overview of Ice Nucleating Particles, Meteorological Monographs, 58, 1.1–1.33,
787 https://doi.org/10.1175/AMSMONOGRAPHS-D-16-0006.1, 2017.

788 Kanji, Z. A., Sullivan, R. C., Niemand, M., DeMott, P. J., Prenni, A. J., Chou, C., Saathoff, H.,
789 and Möhler, O.: Heterogeneous ice nucleation properties of natural desert dust particles coated
790 with a surrogate of secondary organic aerosol, Atmospheric Chemistry and Physics, 19, 5091–
791 5110, https://doi.org/10.5194/acp-19-5091-2019, 2019.

792 Kiselev, A., Bachmann, F., Pedevilla, P., Cox, S. J., Michaelides, A., Gerthsen, D., and Leisner,
793 T.: Active sites in heterogeneous ice nucleation—the example of K-rich feldspars, Science, 355,
794 367–371, https://doi.org/10.1126/science.aai8034, 2017.

795 Knopf, D. A. and Koop, T.: Heterogeneous nucleation of ice on surrogates of mineral dust,
796 Journal of Geophysical Research: Atmospheres, 111, https://doi.org/10.1029/2005JD006894,
797 2006.

798 Kulkarni, G., Sanders, C., Zhang, K., Liu, X., and Zhao, C.: Ice nucleation of bare and sulfuric
799 acid-coated mineral dust particles and implication for cloud properties, Journal of Geophysical
800 Research: Atmospheres, 119, 9993–10011, https://doi.org/10.1002/2014JD021567, 2014.

801 Kumar, A., Marcolli, C., and Peter, T.: Ice nucleation activity of silicates and aluminosilicates
802 in pure water and aqueous solutions – Part 3: Aluminosilicates, Atmospheric Chemistry and
803 Physics, 19, 6059–6084, https://doi.org/10.5194/acp-19-6059-2019, 2019a.

804 Kumar, A., Marcolli, C., and Peter, T.: Ice nucleation activity of silicates and aluminosilicates
805 in pure water and aqueous solutions – Part 2: Quartz and amorphous silica, Atmospheric
806 Chemistry and Physics, 19, 6035–6058, https://doi.org/10.5194/acp-19-6035-2019, 2019b.

807 Kumar, A., Marcolli, C., Luo, B., and Peter, T.: Ice nucleation activity of silicates and
808 aluminosilicates in pure water and aqueous solutions – Part 1: The K-feldspar microcline,
809 Atmospheric Chemistry and Physics, 18, 7057–7079, https://doi.org/10.5194/acp-18-7057-
810 2018, 2018.

811 Marcolli, C., Gedamke, S., Peter, T., and Zobrist, B.: Efficiency of immersion mode ice
812 nucleation on surrogates of mineral dust, Atmospheric Chemistry and Physics, 7, 5081–5091,
813 https://doi.org/10.5194/acp-7-5081-2007, 2007.

814 McGraw, Z., Storelvmo, T., Polvani, L. M., Hofer, S., Shaw, J. K., and Gettelman, A.: On the
815 Links Between Ice Nucleation, Cloud Phase, and Climate Sensitivity in CESM2, Geophysical
816 Research Letters, 50, e2023GL105053, https://doi.org/10.1029/2023GL105053, 2023.

https://doi.org/10.5194/egusphere-2025-6368
Preprint. Discussion started: 18 February 2026

Mignani, C., Wieder, J., Sprenger, M. A., Kanji, Z. A., Henneberger, J., Alewell, C., and Conen, F.: Towards parameterising atmospheric concentrations of ice-nucleating particles active at moderate supercooling, Atmospheric Chemistry and Physics, 21, 657–664, https://doi.org/10.5194/acp-21-657-2021, 2021.

Murray, B. J., Carslaw, K. S., and Field, P. R.: Opinion: Cloud-phase climate feedback and the importance of ice-nucleating particles, Atmospheric Chemistry and Physics, 21, 665–679, https://doi.org/10.5194/acp-21-665-2021, 2021.

Murray, B. J., O'Sullivan, D., Atkinson, J. D., and Webb, M. E.: Ice nucleation by particles immersed in supercooled cloud droplets, Chemical Society Reviews, 41, 6519–6554, https://doi.org/10.1039/c2cs35200a, 2012.

Murray, B. J., Broadley, S. L., Wilson, T. W., Atkinson, J. D., and Wills, R. H.: Heterogeneous freezing of water droplets containing kaolinite particles, Atmospheric Chemistry and Physics, 11, 4191–4207, https://doi.org/10.5194/acp-11-4191-2011, 2011.

Niedermeier, D., Shaw, R. A., Hartmann, S., Wex, H., Clauss, T., Voigtländer, J., and Stratmann, F.: Heterogeneous ice nucleation: exploring the transition from stochastic to singular freezing behavior, Atmospheric Chemistry and Physics, 11, 8767–8775, https://doi.org/10.5194/acp-11-8767-2011, 2011a.

Niedermeier, D., Hartmann, S., Clauss, T., Wex, H., Kiselev, A., Sullivan, R. C., DeMott, P. J., Petters, M. D., Reitz, P., Schneider, J., Mikhailov, E., Sierau, B., Stetzer, O., Reimann, B., Bundke, U., Shaw, R. A., Buchholz, A., Mentel, T. F., and Stratmann, F.: Experimental study of the role of physicochemical surface processing on the IN ability of mineral dust particles, Atmospheric Chemistry and Physics, 11, 11131–11144, https://doi.org/10.5194/acp-11-11131-2011, 2011b.

Peckhaus, A., Kiselev, A., Hiron, T., Ebert, M., and Leisner, T.: A comparative study of K-rich and Na/Ca-rich feldspar ice-nucleating particles in a nanoliter droplet freezing assay, Atmospheric Chemistry and Physics, 16, 11477–11496, https://doi.org/10.5194/acp-16-11477-2016, 2016.

Perkins, R. J., Gillette, S. M., Hill, T. C., and DeMott, P. J.: The labile nature of ice nucleation by Arizona Test Dust, ACS Earth and Space Chemistry, 4, 133–141, https://doi.org/10.1021/acsearthspacechem.9b00304, 2019.

Salam, A., Lesins, G., and Lohmann, U.: Laboratory study of heterogeneous ice nucleation in deposition mode of montmorillonite mineral dust particles aged with ammonia, sulfur dioxide, and ozone at polluted atmospheric concentrations, Air Quality, Atmosphere & Health, 1, 135–142, https://doi.org/10.1007/s11869-008-0019-6, 2008.

Salam, A., Lohmann, U., and Lesins, G.: Ice nucleation of ammonia gas exposed montmorillonite mineral dust particles, Atmospheric Chemistry and Physics, 7, 3923–3931, https://doi.org/10.5194/acp-7-3923-2007, 2007.

Savre, J. and Ekman, A. M. L.: A theory-based parameterization for heterogeneous ice nucleation and implications for the simulation of ice processes in atmospheric models, Journal

https://doi.org/10.5194/egusphere-2025-6368
Preprint. Discussion started: 18 February 2026

of Geophysical Research: Atmospheres, 120, 4937–4961, https://doi.org/10.1002/2014JD023000, 2015.

Sullivan, R. C., Petters, M. D., DeMott, P. J., Kreidenweis, S. M., Wex, H., Niedermeier, D., Hartmann, S., Clauss, T., Stratmann, F., Reitz, P., Schneider, J., and Sierau, B.: Irreversible loss of ice nucleation active sites in mineral dust particles caused by sulphuric acid condensation, Atmospheric Chemistry and Physics, 10, 11471–11487, https://doi.org/10.5194/acp-10-11471-2010, 2010.

Tobo, Y., DeMott, P. J., Raddatz, M., Niedermeier, D., Hartmann, S., Kreidenweis, S. M., Stratmann, F., and Wex, H.: Impacts of chemical reactivity on ice nucleation of kaolinite particles: A case study of levoglucosan and sulfuric acid, Geophysical Research Letters, 39, https://doi.org/10.1029/2012GL053007, 2012.

Vali, G. and Snider, J. R.: Time-dependent freezing rate parcel model, Atmospheric Chemistry and Physics, 15, 2071–2079, https://doi.org/10.5194/acp-15-2071-2015, 2015.

Welti, A., Lüönd, F., Kanji, Z., Stetzer, O., and Lohmann, U.: Time dependence of immersion freezing: an experimental study on size selected kaolinite particles, Atmos Chem Phys, 12, 9893–9907, https://doi.org/10.5194/acp-12-9893-2012 2012.

Wex, H., DeMott, P., Tobo, Y., Hartmann, S., Rösch, M., Clauss, T., Tomsche, L., Niedermeier, D., and Stratmann, F.: Kaolinite particles as ice nuclei: learning from the use of different kaolinite samples and different coatings, Atmospheric Chemistry and Physics, 14, 5529–5546, https://doi.org/10.5194/acp-14-5529-2014, 2014.

Wright, T. P. and Petters, M. D.: The role of time in heterogeneous freezing nucleation, Journal of Geophysical Research: Atmospheres, 118, 3731–3743, https://doi.org/10.1002/jgrd.50365, 2013.

Zolles, T., Burkart, J., Häusler, T., Pummer, B., Hitzenberger, R., and Grothe, H.: Identification of ice nucleation active sites on feldspar dust particles, The Journal of Chemical Physics, 119, 2692–2700, https://doi.org/10.1021/jp509839x, 2015.